

PAPER

Crosslinked network microstructure of carbon nanomaterials promotes flaw-tolerant mechanical response

To cite this article: Jamshid Kavosi *et al* 2020 *Nanotechnology* **31** 315606

View the [article online](#) for updates and enhancements.

You may also like

- [Embedding Co₃P nanoparticles in Cu doping carbon fibers for Zn-air batteries and supercapacitors](#)
Xingwei Sun, Haiou Liang, Haiyan Yu et al.
- [Stretched lignin/polyacrylonitrile blended carbon nanofiber as high conductive electrode in electric double layer capacitor](#)
Manish Kumar, Shogo Taira, Nutthira Pakkang et al.
- [Enhanced microwave absorption property of epoxy nanocomposites based on PANI@Fe₃O₄@CNFs nanoparticles with three-phase heterostructure](#)
Lingfeng Yang, Haopeng Cai, Bin Zhang et al.



244th ECS Meeting

Gothenburg, Sweden • Oct 8 – 12, 2023

Early registration pricing ends
September 11

Register and join us in advancing science!

[Learn More & Register Now!](#)



Crosslinked network microstructure of carbon nanomaterials promotes flaw-tolerant mechanical response

Jamshid Kavosi¹ , Terry S Creasy¹, Alan Palazzolo² and Mohammad Naraghi^{1,3} 

¹ Department of Materials Science and Engineering, Texas A&M University, 3409 TAMU, College Station, TX 77843-3409, United States of America

² Department of Mechanical Engineering, Texas A&M University, 3409 TAMU, College Station, TX 77843-3409, United States of America

³ Department of Aerospace Engineering, Texas A&M University, 3409 TAMU, College Station, TX 77843-3409, United States of America

E-mail: naraghi@aero.tamu.edu

Received 8 January 2020, revised 4 April 2020

Accepted for publication 21 April 2020

Published 20 May 2020



Abstract

Carbon nanomaterials, such as carbon nanotubes (CNTs) and carbon nanofibers (CNFs), are chemically inert in their highly graphitic forms. Various post processing methods can activate their surfaces to enhance their interactions with a host matrix in a nanocomposite. Chemical surface functionalization is used often. This method however can lead to major strength loss in nanomaterials stemming from induced surface defects (changing sp^2 bonds to sp^3 bonds). In this manuscript, we have experimentally studied the mechanical properties of the individual, pyrolysis-fabricated CNFs. These CNFs have a highly crosslinked 3D network of C–C bonds. The strength of CNFs has been studied as a function of O/C ratio. The loss in strength due to functionalization has been compared to that of other carbon nanomaterials with layered structures (CNT and graphene). Comparisons were also made with carbon microfibers. Fracture strength estimations of the critical flaw size in CNFs, CNTs and graphene were also made. The results revealed that despite having high surface area, carbon nanomaterials with crosslinked microstructure are resilient to flaws as big (deep) as 10–30 nm, while nanomaterials with layered structure (such as CNTs) experience a dramatic loss in strength with much lower flaw sizes. Hence, it seems that graphitic nanomaterials such as graphene and CNT have high strength that, although higher than CNFs, comes at a cost to flaw tolerance and robustness. Since failure is often progressive, this work demonstrates a benefit that crosslinked nanomaterials have over highly graphitic ones, such as CNTs, in load bearing applications.

Supplementary material for this article is available [online](#)

Keywords: carbon nanofibers, functionalization, nanomechanics, flaw tolerance

1. Introduction

Carbon nanomaterials such as carbon nanotubes (CNTs), carbon nanofibers (CNFs) and graphene nanoplatelets (GNPs) maybe employed as nanofiller to other materials, such as polymers, to enhance mechanical properties. These efforts are motivated by nanomaterial's remarkable properties, such

as strength and modulus as high as 100 GPa and 1 TPa, respectively, for graphene and CNTs [1–4]. The reported relative improvements in mechanical properties are amazing. For instance, adding just 0.01 wt% of functionalized graphene sheets to poly(methyl methacrylate) (PMMA) has led to a 33% increase in elastic modulus compared to the base polymer, far exceeding the rule of mixture predictions [5]. A

more recent example has measured 14% improvement in strength by adding only 0.5 wt. % functionalized CNTs to epoxy [6].

While relative improvement in properties by adding carbon nanofillers is impressive, the carbon nanofillers content in nanocomposites is often below 2 wt.% [7, 8]. Only in rare cases, higher nanofiller loadings have been studied [9, 10]. This is mainly due to agglomerated nanoparticles or poor nanofiller wettability by the matrix that adversely affects load transfer between fillers and matrix [6, 8].

An effective approach to reduce agglomeration is to functionalize the surface of the nanofiller. This approach not only enhances the filler's dispersion in the matrix during processing (often from liquid phase in a solvent, melt or pre-cured epoxy), but also increases the load transfer between the filler and matrix in the cured phase via for instance forming covalent bonds between the filler and matrix and mechanical interlocking (caused by inducing surface undulations in nanomaterials) [6, 11–13]. However, in carbon nanomaterials, chemical functionalization changes the surface bond types, from sp^2 hybridized C–C bond (graphitic bonds) to sp^3 bonds to accommodate the functional groups. An unintended consequence of that is a drop in mechanical strength, as the sp^3 bonds act as defects [14, 15]. For certain defects, such as vacancies in graphene, the drop-in strength can be significant, claiming more than 60% of the pristine material's strength [16]. The defects include the C atoms around vacancies or voids in the material, from where the cracks will start [14, 17].

The loss in carbon nanomaterial strength can be explained based on size effects. The high surface to volume ratio in nanomaterials increases the overall contribution that surface defects have on strength [16]. While in carbon nanomaterials, functionalization always reduces the filler's strength, in carbon microfibers, mild functionalization may not affect the strength or may even remove surface flaws and increase the strength [18, 19]. Moreover, the drop in strength with oxidation in nanomaterials with layered structures such as CNTs and GNP (and Graphene) can be even more intense. That is because the load transfer from the matrix to the filler occurs in the outmost layer (a single atomic thick layer), and chemical functionalization-induced defects will disrupt the load path within this layer. Hence, using functionalized carbon nanofillers to improve nanocomposite mechanical properties brings tradeoffs between (a) improvement in dispersion and load transfer between filler and matrix, and (b) reduction in filler load bearing (mechanical) properties.

A remedy for the above problem is sought in an emerging carbon nanomaterials class where the covalent bonds within the nanofiller are not limited to a plane. This category is carbon nanofibers (CNFs) that are formed by pyrolyzing polymeric precursors [20–24]. Unlike CNTs and GNPs with layered structure (with in plane covalent bonds) and weak van-der-Waals interactions between layers, the CNF microstructure consists of a crosslinked amorphous carbon and turbostratic layer network. However, given the high surface to volume ratio, which is inherent to all nanomaterials, it is not clear whether an optimum defect density/surface

functionalization exists in CNFs that can enhance nanomaterial dispersion within a matrix without considerable loss in nanofiller strength.

To address this knowledge gap, we studied the surface morphology, chemistry, and mechanical properties for individual, surface-functionalized CNFs followed by the mechanically testing CNFs epoxy coupons. The studies included characterizing individual CNFs mechanically with respect to surface functionalization and performing fracture mechanics analysis. Epoxy composite with both pristine and functionalized CNFs were fabricated and mechanically tested. Fracture mechanics estimates of critical flaw sizes were presented to further shed light on the experimentally measured values. Finally, the CNF composites mechanical properties were related to the CNFs and interface properties. The experiments at two length scales, the scale of individual CNFs and of their composites, provided valuable knowledge about the role the filler interface has on nanocomposite mechanics.

2. Experimental

2.1. Fabricating electrospun carbon nanofibers

Carbon nanofibers (CNFs) were fabricated by thermally stabilizing and carbonizing electrospun polyacrylonitrile (PAN) nanofibers. The overall approach is presented in our earlier works [22] with minor changes as presented here. PAN powder with an average molecular weight of $M_w = 150\,000\text{ g mol}^{-1}$ was dissolved in N,N-dimethylformamide (DMF) and magnetically stirred for 24 h at room temperature to obtain a 10 wt.% solution. The raw materials were obtained from Sigma-Aldrich. The continuous PAN nanofibers landed on the electrically grounded roller, forming a nearly unidirectional fiber mat. The rotating collector's tip velocity was $\sim 1\text{ m s}^{-1}$. The electrospinning voltage was 25 kV, and the needle-to-collector distance was set to 20 cm.

PAN nanofiber mats stretched under hanging weights equivalent to $\sim 19\text{ MPa}$ engineering stress as the mats heated from $100\text{ }^\circ\text{C}$ – $135\text{ }^\circ\text{C}$ to achieve a drawing ratio of 2. This draw ratio came from previous research studies that nearly doubled CNF strength while leading to insignificant adhesion between them [8]. The hot-drawn PAN nanofibers were thermally stabilized in a convection oven by heating from room temperature to $275\text{ }^\circ\text{C}$ at $5\text{ }^\circ\text{C min}^{-1}$ (2 h hold time at the peak temperature), and carbonized at a $1400\text{ }^\circ\text{C}$ peak temperature in a tube furnace for (1 h hold time at the peak temperature) in an inert nitrogen atmosphere.

2.2. Functionalizing the CNF surface

CNF surface functionalization occurred in concentrated HNO_3 (68 wt%). To this end, a CNF ribbon was collected on the Teflon (PTFE) clips and immersed in nitric acid at $100\text{ }^\circ\text{C}$ for 15, 30, 60, and 120 min durations. The acid treatment conditions were partly adopted from Bahl *et al* [19]. Concentrated nitric acid was obtained from Sigma-Aldrich. Following this step, surface-functionalized CNFs received a distilled

water rinse until they reached *pH* value between 5.5–6.5; subsequently, the nanofibers were dried at 60 °C for ~4 h.

2.3. Mechanical and material characterization of CNFs

The pristine (as-fabricated) CNFs and surface functionalized CNFs underwent material and mechanical characterization. The CNFs diameters were measured by imaging them in SEM. At least 35 samples were tested for each fabrication condition, to obtain a statistically reliable diameter distribution. The CNFs surface chemistry was analyzed via x-ray photoelectron spectroscopy (XPS) using an Omicron XPS/UPS system with an Argus detector relying on dual Mg/Al x-ray source (Scienta Omicron GmbH, Taunusstein, Germany). Acid functionalization effects were also studied by Fourier Transform IR (FTIR) spectroscopy. For this purpose, Thermo Nicolet 380 FTIR spectrometer with a manual infrared (IR) polarizer obtained from PIKE Technologies was employed. Individual CNFs mechanical properties were also measured via micromachined tension test devices. At least four measurements was performed for each fabrication condition. Details about the mechanical testing devices of individual CNFs and the measurement approach is presented in our earlier work [22, 25].

2.4. Fabricating and characterizing CNF nanocomposites

Surface functionalization should in principle support load transfer between the CNFs and a conventional polymer matrix such as epoxies via combined dispersive and covalent bonds. To evaluate and quantify the effect surface functionalization has on the nanocomposite mechanics, CNF-epoxy nanocomposites were fabricated following the procedure described by Gardea *et al* [26] with minor adjustments. This procedure is tuned to partially cure the epoxy while the CNF-epoxy is mixed, to increase the mixture viscosity and to prevent CNFs agglomeration.

In this study, we used EPIKOTE™ resin 862 (Bisphenol-F epoxy resin) with EPIKURE™ curing agent W. To prepare the nanocomposites, the CNF mats were cut to 0.5 cm long pieces and then dispersed in the 20 ml of ethanol with ultrasonic bath for 80 min. Immediately after, the CNFs/solvent solution with 20 ml extra ethanol was added to EPIKOTE™ resin 862 (Bisphenol-F (BPF) epoxy resin). The appropriate curing agent amount (EPIKURE™ curing agent W) was set (100:26.4 by weight) as provided by the manufacturer in two steps. The first 20% of the required curing agent was added to the solution and magnetically stirred at 500 rpm at 120 °C for 3 h. This step increases the solution viscosity to prevent CNF agglomeration. Following this pre-curing step, the solution was cooled to about 80 °C, the remaining curing agent was added, and the mixture degassed at 500 rpm for 30 min. Thereafter, the CNF/epoxy solution was poured into a pre-heated mold at 120 °C with a curing cycle set to 8 h at 40 °C followed by 1 h at 121 °C and another 2.5 h at 177 °C. The first 8 h curing at 40 °C increases the viscosity. This step reduces the thermo-mechanical viscosity drop while curing at higher temperatures, thus, the 40 °C step limits CNF agglomerate

formation. At least five dog-bone samples for each condition following the standard ASTM D638 were fabricated and tested.

3. Results and discussion

3.1. Surface morphology of functionalized CNFs

Pristine and acid functionalized CNF mats were imaged in SEM. Figures 1(a)–(c) present SEM images showing the fibers. As shown, a 15 min surface treatment is insignificant in changing the CNF surface morphology. However, pits and etches on the CNF surface—with an approximate dimension about 10–15 nm along the fiber—are evident after 30 min of acid functionalization. Given the CNFs' heterogeneous structure, composed of partially graphitic domains with various degrees of graphitization and amorphous carbon [27], selective etching in less-graphitic domains on the CNF surface can lead to pitting.

Figures 1(d)–(f) show the CNF diameter distribution before and after acid treatment for 15 and 30 min. The fiber diameter distribution during the early stages is nearly the same. Pristine CNFs are about 103 ± 17 nm diameter, and changed to 101 ± 17 nm and 100 ± 17 nm after 15 and 30 min of acid treatment, respectively. Pit formation in 30-minute treated CNFs indicates surface etching. However, direct and precise diameter changes—down to a few nanometers—resulting from acid functionalization is not feasible here because the diameter has a standard deviation (~17 nm) introduced by bending instability during electrospinning. During the early stages, i.e. the first 15 min, acid treatment has likely removed only the loosely bound hydrocarbons on the CNF surface; those loose hydrocarbons can be a few atomic-layers thick [18, 28]. This is evident in the sharper carbon skeleton peaks in the FTIR spectra after functionalization as presented in the next section.

3.2. Chemically characterizing CNF surfaces

The CNF surface chemistry, the surface functional groups formed, and their relative concentration was studied via FTIR and XPS. The FTIR spectrum for as-fabricated CNFs and acid treated CNFs with different acid treatment durations appears in figure 2. In pristine and functionalized CNFs, a peak was observed at 1520 cm^{-1} , which is assigned to the carbon skeleton [29, 30]. Acid treatment strengthens these peaks and shifts it to higher wavenumber (1575 cm^{-1}). This finding suggests the weakly bonded hydrocarbon layer left the CNF surface during acid treatment.

There is also a peak at 1230 cm^{-1} , corresponding to C–O bond stretching in carboxylic groups, that strengthened upon acid treatment. This peak is observed in both pristine and functionalized samples. Pristine CNFs add oxygen during stabilization and from oxygen impurities present during carbonization. Moreover, in functionalized CNFs, a peak emerges at 1742 cm^{-1} , which is assigned to C=O stretching vibration in carbonyl and carboxyl groups. There is also a broad peak at $3100\text{--}3600\text{ cm}^{-1}$, which is assigned to –OH group in carboxyl

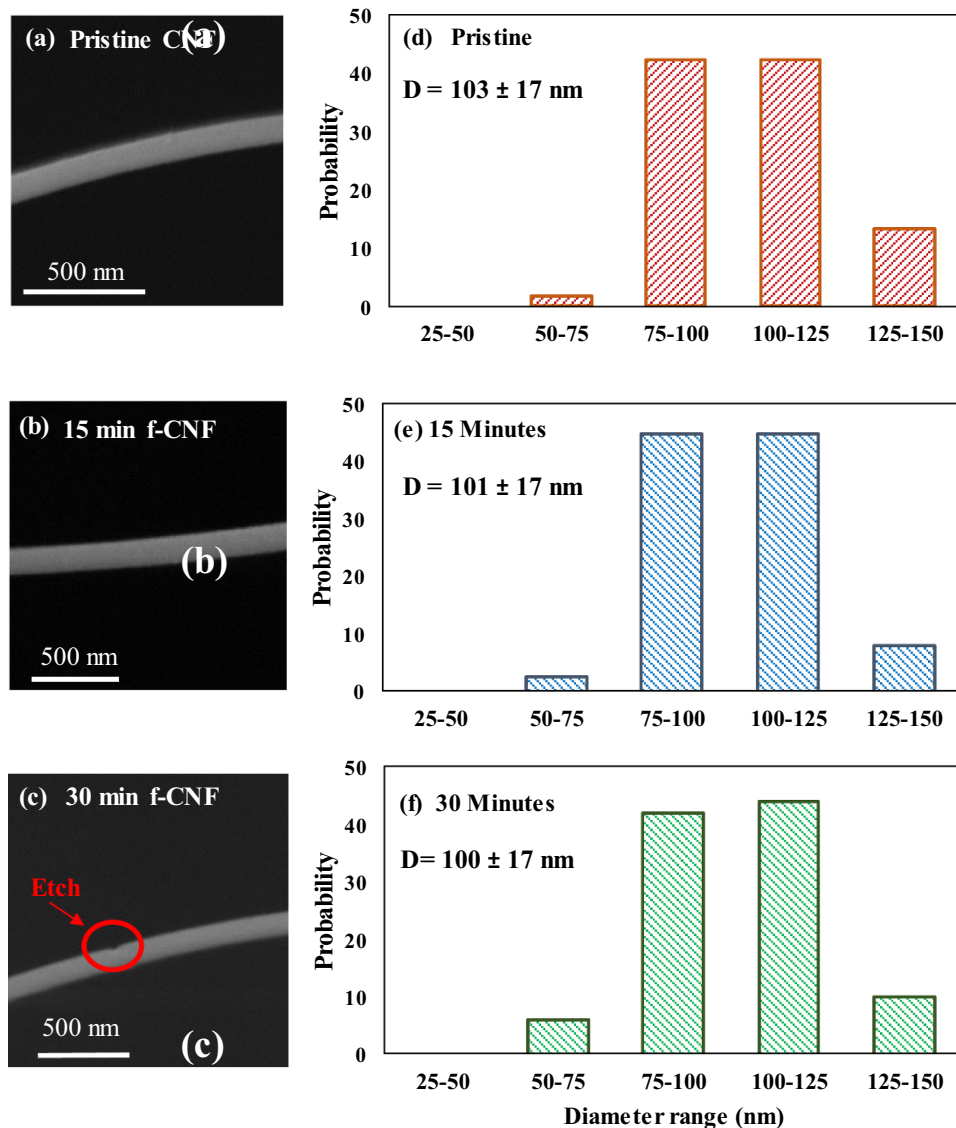


Figure 1. (a)–(c) SEM images showing CNF before and after 15 and 30 min acid functionalization. (d)–(f) The CNF diameter distribution with functionalization time.

and alcohol group [30]. The surface functional groups of the functionalized CNFs are shown schematically in figure 2(b).

Based on the FTIR spectrum, the acid treatment duration effectively controls functionalization intensity. After 60 min nitric acid treatment, the peaks associated with the oxygen moieties are much stronger than those formed in shorter acid treatment durations.

The surface functional groups for pristine and functionalized CNFs were studied further via XPS. The full survey showing pristine CNFs and functionalized CNFs appears in figure S1 (available online at stacks.iop.org/Nano/31/315606/mmedia). The surveys for all CNFs mainly consist of C 1s peak, at a 284.4 eV binding energy, and O 1s, at 532.6 eV binding energy. In functionalized CNFs the O 1s peak is stronger because there is surface oxidation.

High-resolution XPS spectra of C1s provided further information about the functional groups. The C1 s spectrum of XPS for various treatment durations CNFs is shown in

figures 3(a)–(d). The spectra have each been resolved into five individual peaks that represent graphitic carbon (284.4 eV), carbon present in hydroxyl or ethers group (285.9–286.0 eV), carbonyl group (287.4–287.5 eV), carboxyl or ether group (288.5–288.7 eV), and a weak carbonate groups (290.6–290.7 eV).

According to the elemental composition taken from the XPS survey, figure 3(e), the oxidative functionalization after only 15 min acid treatment leads to an 11% atomic oxygen to carbon ratio; this is a ~5 fold increase from 2% in pristine CNFs. However, further acid treatment for 30, 60, and 120 min only slightly increase the oxygen content to 13, 12, 16%, respectively. The increase in oxygen content comes from functional groups such as hydroxyl, carboxyl, and carbonyl groups that form on CNF surfaces. The oxygen absorption rate reduces after 15 min treatment by almost an order of magnitude. This is expected because, in the early treatment stage, surface oxidation may lead to oxidized graphitic domain edges

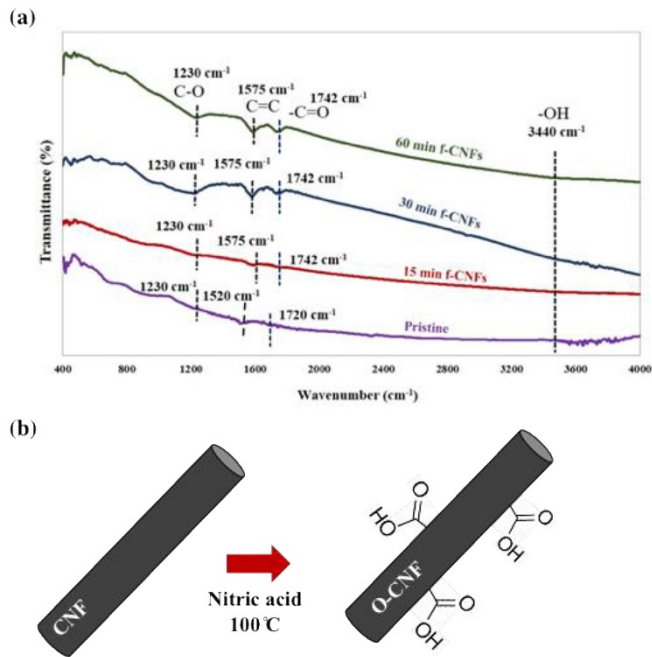


Figure 2. (a) schematic of the acid functionalization with nitric acid and grafting of the functional group on its surface. (b) FT-IR spectra before and after CNFs receive acid treatment for 15, 30, and 60 min.

on the CNF surface. As the number of un-oxidized edges available drops over time, the oxidation rate falls.

Based on the spectra shown in the figures 3(a)–(d), carbonyl and carboxyl group percentages increase abruptly during the first 15 min during acid functionalization, followed by a moderate increase after longer acid treatments. The overall alcohol group percentages did not change substantially during acid functionalization. This data suggests that hydroxyl groups (–OH) formed on the CNF surface during acid functionalization are consumed to form –COOH and C=O groups [31], figure 3(f). Hence, progressive exposure to aqueous nitric acid increasingly enriches CNFs surface with oxygen moieties, specifically carbonyl and carboxyl groups.

3.3. Mechanical properties of CNFs as a function of O/C contents

As discussed in the introduction, chemical functionalization may adversely affect strength in carbon nanomaterials by disrupting graphitic bonds. Unlike nanomaterials such as CNTs and GNP with layered structure [14–16], the highly cross-linked C bond network within the CNFs' structure, obtained via pyrolyzing and crosslinking the precursor polymer chains, may make the material more resistant to flaws that are induced via chemical functionalization. This is because their crosslinked network structure will provide load transfer path around surface flaws. To evaluate this phenomenon, we studied CNF mechanical properties at three functionalization conditions: (i) as fabricated CNFs, i.e. no acid functionalization, (ii) after 15 min and (iii) 30 min functionalization. Single CNF nanofiber mechanical properties before and after acid

treatment were characterized by using a MEMS-based nano-mechanical testing platform. Individual CNFs were mounted on MEMS device with 3D-manipulator controlled sharpened tungsten tip. Tescan LYRA-3 focused ion beam (FIB) is used to deposit platinum (Pt) block on it to fix it on device. The stage is actuated to load individual nanofibers under an optical microscope. By applying Digital Image Correlation to calculate the displacement of different platforms of the MEMS device, and by knowing the stiffness of the load cell, the stress–strain curve of individual CNF tensile test is obtained. More details about the testing device can be found in previous works [27, 32, 33].

Representative CNF stress–strain curves appear in figure 4(a). As shown in the figure, in all tested cases, the CNF mechanical behavior is linear elastic up to failure. Figure 4(b) presents an SEM image showing a CNF tested in tension using the MEMS device. A close-up image revealing the fracture surface appears in an insert within figure 4(b). The average modulus and strength values appear in figures 4(c) and (d), respectively.

Comparing the mechanical properties of as-spun CNFs carbonized at 1400 °C with those fabricated at 1100 °C [34] it becomes clear that higher carbonization temperatures lead to higher strength and modulus. In addition, the values we reported for strength is higher than those previously reported by [24, 25], indicating the contribution of precursor hot-drawing (employed in the present study) to enhance strength of CNFs.

While the average tensile strength and modulus for CNFs during the 15 min acid functionalization are approximately unchanged—within the measurement's uncertainty—the scatter in the measured strength and modulus drops considerably (by ~50% or more). This is potentially due to surface defects—such as the loosely bound layer of hydrocarbons on the surface—getting removed during early functionalization.

However, further acid treatment for 30 min led to more than 50% decrease in the strength and modulus. SEM images provide insights into the cause. As shown in figures 1(c) and 4(b) insert, extended acid treatment forms pits and voids on the CNF surface. These are likely the locations along the CNFs with lower graphitization—locations that were removed selectively via acid treatment. In all 30-minute acid treated CNFs, we observed at least one pit in the gage length for every case, suggesting a linear density with more than 1 defect with a characteristic length (pit depth or length) of ~10–15 nm.

It is illustrative to compare strength loss in CNFs with the strength lost in carbon fibers after similar acid treatment. While CNFs lost ~50% after 30 min acid treatment at 100 °C, similar treatments only reduce carbon fiber strength by ~7% [35]. This indicates the pronounced effect surface modifications have on the CNF strength compared to carbon fibers because the CNFs have much higher surface to volume ratio. In other words, a surface flaw with measuring ~10 nm, as shown in figure 1(c) insert, has a more pronounced effect on a ~120 nm thick CNF than on a 5 μm thick carbon fiber. The higher specific area of carbon nanofibers means that the number of active sites per fiber unit volume where flaws can form is higher than in regular carbon fiber. Hence, CNFs are more sensitive to acid treatment compared to carbon fibers.

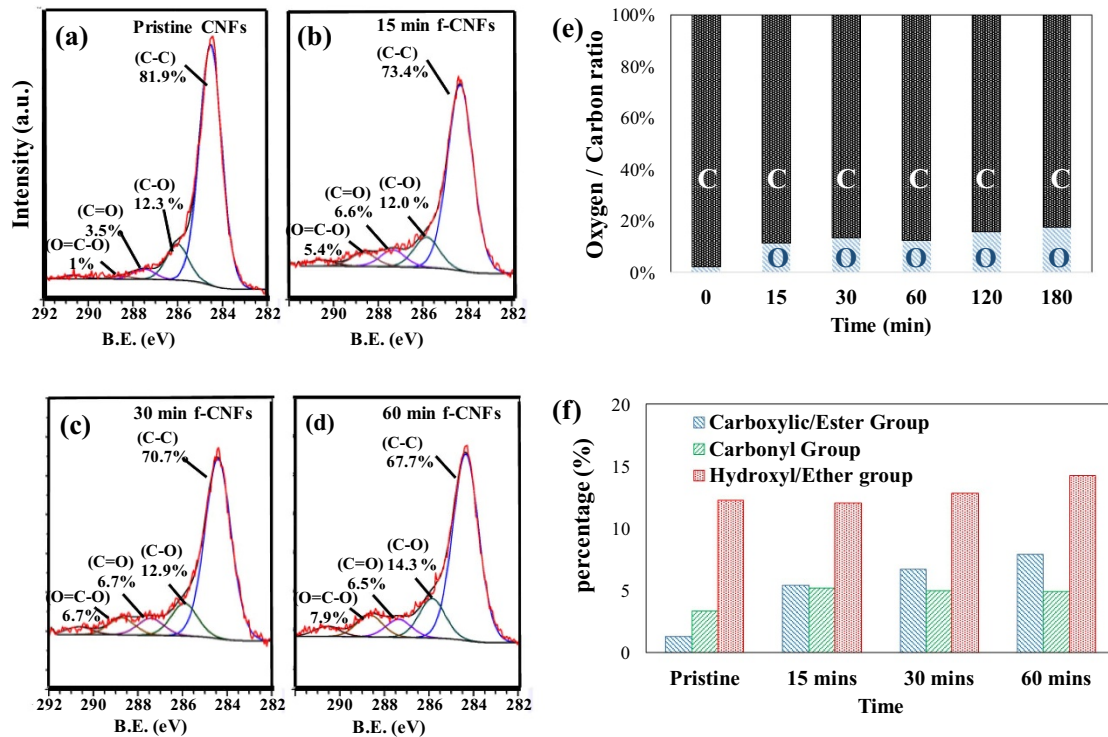


Figure 3. (a)–(d): CNFs carbon 1s spectra after 0, 15, 30, and 60 min acid functionalization, (e) relative oxygen to carbon ratio of CNFs at different acid functionalization times (f) relative contribution from each functional group in the CNF C 1s spectrum.

This is attributed to the higher surface to volume ratio in nanomaterials, that means the surface defect density will be higher for the same acid treatment conditions.

The changes in CNFs mechanical properties in conjunction with their surface morphology during acid functionalization appears in figure 5. In this figure, the horizontal axis is the atomic ratio for oxygen to carbon, O/C, which measures oxidation progress, as obtained from XPS results in section 3.2. As mentioned earlier, the oxygen absorption rate in CNFs increases abruptly in the first few minutes during acid functionalization, followed by a moderate increase for the longer exposure to nitric acid. This jump comes at a negligible decrease in tensile strength, although the difference between the two cases is within the uncertainty of the measurement—a favorable condition for wettability of CNFs inside a matrix. However, further acid treatment can only marginally increase the oxygen-containing groups on the surface, while it drastically lowers strength by inducing surface defects. A fracture analysis study provides further insights into CNFs flaw resilience relative to other C-based nanomaterials.

3.4. Insights into CNF flaw-resilience from fracture mechanics

As shown in the previous section, a measurable reduction in CNF strength with functionalization is observed only when the surface flaws (e.g. the depth of the surface pits) have grown to ~30–50 nm. In other words, there seems to exist a critical flaw size; the strength is insensitive to flaws smaller than the critical size. Following a similar argument as present in [36, 37], this

critical flaw size can be explained as follows. According to the Griffith criterion, the fracture strength of a sample σ_f with a flaw size of a can be approximated as [36]

$$\sigma_f = \alpha \sqrt{\frac{EG_c}{a}} \quad (1)$$

where E , G_c and α are respectively the elastic modulus and surface energy of the nanofiber and α is a proportionality constant. Ignoring the CNF surface curvature (i.e., defect size much smaller than CNF diameter), α is close to $1/\sqrt{\pi}$. For the CNFs to be insensitive to flaws (such as pits that form on the surface), the flaw size a should be smaller than or equal to a critical flaw size $a_{critical}$ such that the fracture strength becomes equal to the theoretical strength (σ_{theory} , the material's strength without any cracks). Setting $\sigma_f = \sigma_{theory}$ and expressing surface energy in terms of the critical stress intensity factor for mode I failure as $G_c = K_{IC}^2/E$, the critical flaw size can be estimated as

$$a_{critical} = \frac{1}{\alpha^2} \left(\frac{K_{IC}}{\sigma_{theory}} \right)^2 \quad (2)$$

Setting $K_{IC} \approx 1 \text{ MPa}\sqrt{\text{m}}$ from [38], $\sigma_{theory} \sim 5.51 \pm 2.1 \text{ GPa}$ (from tests on unfunctionalized CNFs), and $\alpha^2 \sim 1/\pi$, the critical flaw size can be estimated as $a_{critical} \approx 16 \pm 10 \text{ nm}$. It is indeed rewarding to note that flaw sizes larger than this critical value were observed in the 30 min functionalized samples where a major drop in strength was observed (figures 1(c) and 4(d)), while no such large surface defects and consequently negligible drop in strength was observed in the 15 min functionalized CNFs.

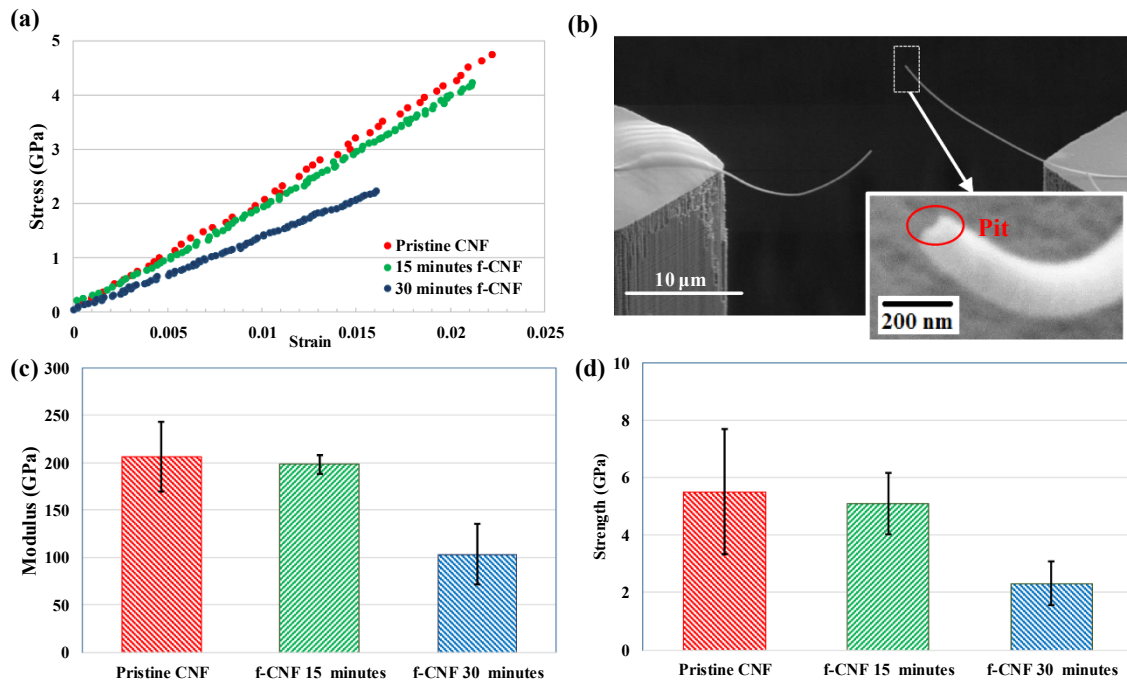


Figure 4. (a) Representative stress-strain curve for the pristine, 15 min functionalized CNF, and 30 min functionalized CNF, (b) 30 min functionalized carbon nanofiber mounted on the MEMS device after nano-mechanical testing, insert shows the fracture surface with the etch on the surface, (c) CNF tensile strength versus functionalization time, (d) CNF tensile modulus versus functionalization time.

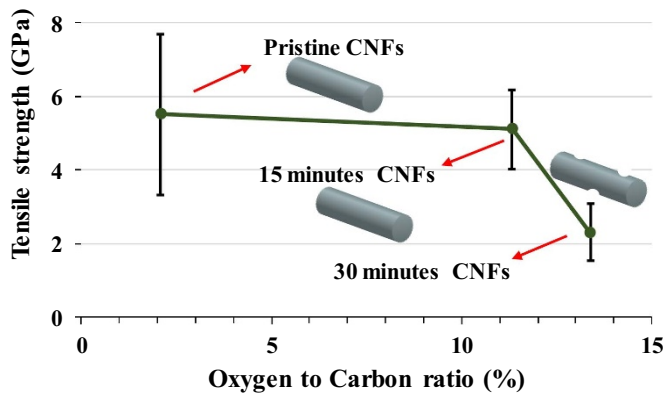


Figure 5. CNF tensile strength versus O/C ratio for three functionalization conditions.

It is illustrative to compare the critical flaw size in CNFs with those in other carbon nanomaterials such as graphene. In graphene, the critical stress intensity factor for mode I failure is measured to be $K_{IC} \approx 4 - 6 \text{ MPa}\sqrt{m}$ and strength for graphene with no cracks can reach 40 GPa [39]. Therefore, according to equation (2) the critical flaw size in graphene is $\sim 3-5 \text{ nm}$. Comparable or even smaller critical flaw size can also be estimated for CNTs by using the reported theoretical strength and fracture toughness for CNTs [40–42]. Thus, it seems that the critical flaw size in CNTs and graphene is much lower than for CNFs.

In this comparison, one has to note the major differences in the microstructures. CNFs are composed of less graphitic structures. In other words, it seems that the remarkable strength in highly graphitic nanomaterials such as graphene comes at

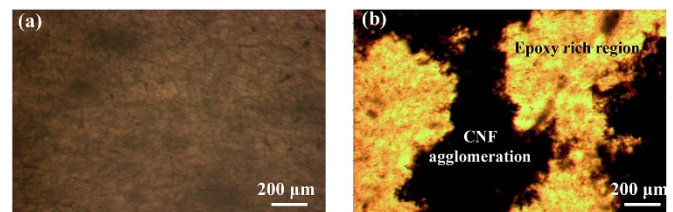


Figure 6. Effect of additional step slow curing at 40 °C for 8 h on dispersion of CNFs within the epoxy: (a) composite containing 1 wt% functionalized CNFs with low temperature hold (b) composite containing 1 wt% functionalized CNFs without low temperature hold shows agglomerations.

a cost to flaw tolerance and structural robustness. The latter should be given major consideration in nanomaterials when using them for load bearing application. That is because failure is often progressive and starts from the weakest link. This consideration may help refocus the research on nanomaterials towards fabrication processes where defects are more controllable, such as pyrolysis [32].

3.5. CNFs/epoxy composite mechanical behavior

To evaluate the effect surface functionalization has on CNFs mechanical properties in the CNF-epoxy nanocomposites, nanocomposites with 1 wt% pristine CNFs and 1 wt% functionalized CNFs were fabricated and subjected to mechanical characterization. The surface functionalization was limited to 15 min to minimize defect formation on CNFs. To improve dispersion, the epoxy's curing profile was modified to reduce

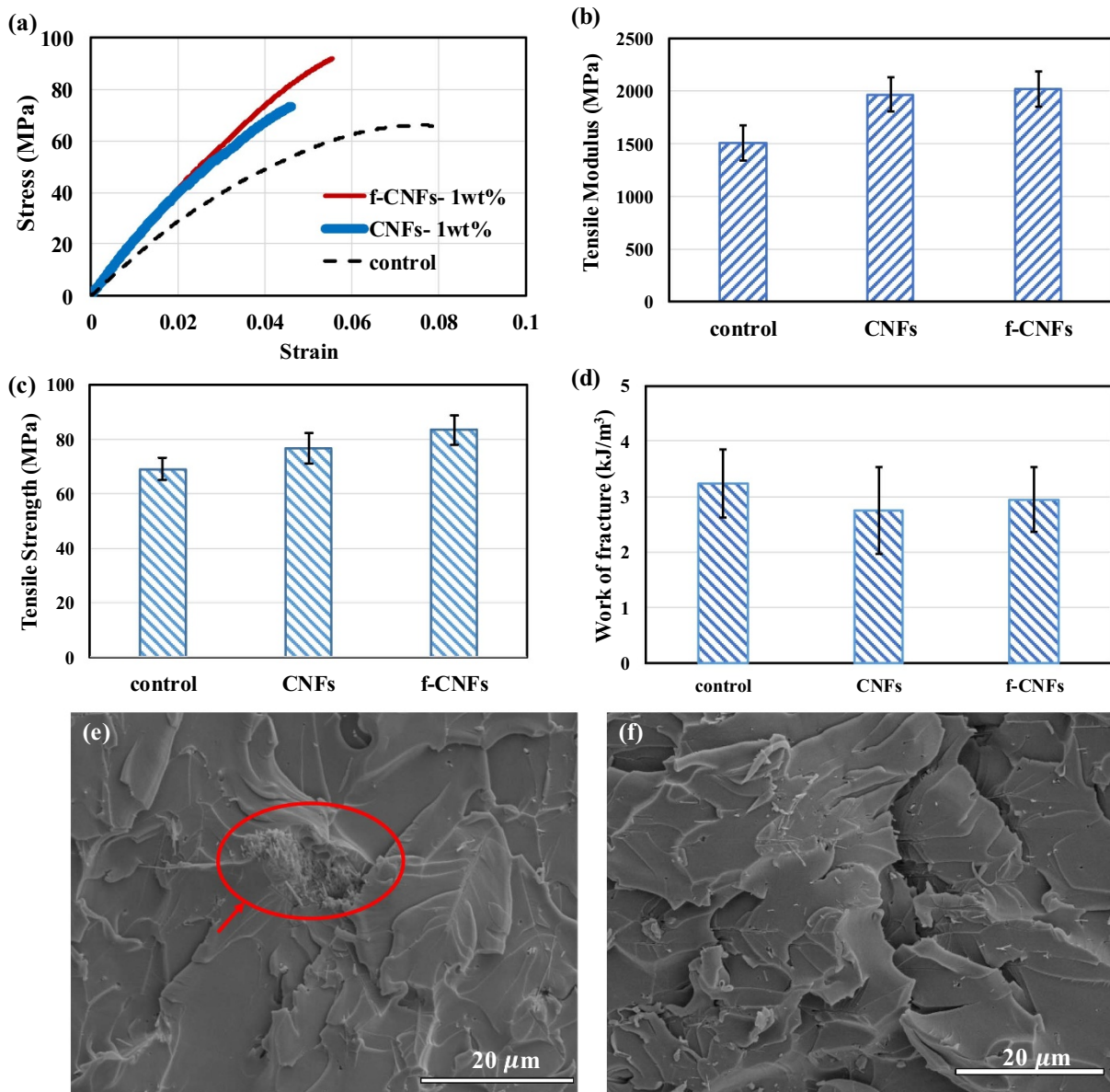


Figure 7. (a) Stress–strain behavior for the epoxy, 1 wt.% pristine CNFs/epoxy composite, and 1 wt.% functionalized CNFs/epoxy composite and (b) elastic modulus, (c) tensile strength, (d) energy to failure of the 1 wt.% pristine and functionalized carbon nanofibers/epoxy composite (e) and (f) SEM image shows the fracture surface in the composite specimen containing 1 wt% pristine and functionalized CNFs.

CNF mobility during, as discussed in the experimental section. The CNF dispersion in cured epoxy was evaluated under an optical microscope. The curing profile for all the samples subjected to mechanical tests includes heating for 8 h at 40 °C followed by 1 h at 121 °C and another 2.5 h at 177 °C. This curing profile led to a good CNF dispersion within the epoxy is obvious from optical images in figure 6(a). A subtle but critical step in the curing cycle is the preheating for 8 h at 40 °C. This step gradually increases the epoxy viscosity by crosslinking at a low temperature where an drop in viscosity from thermo-physical effects is negligible. This step is significant in improving the dispersion of CNFs as shown in the optical images from samples made without this step where massive CNFs agglomeration appears, figure 6(b).

Dog bone samples were tested in tension and their mechanical properties were evaluated. The mechanical characterization used only samples obtained from the modified curing cycle with good CNF dispersion evaluated from optical microscope. Example stress-strain curves for neat epoxy, and epoxy reinforced with functionalized and un-functionalized (pristine) CNFs appear in figure 7(a). Figure 7(b)–(d) show tensile strength, modulus, and energy to failure (area under the stress strain curve) for various samples, respectively.

As shown in figure 7, adding 1 wt% pristine CNFs (unfunctionalized) to the epoxy led to a considerable increase in modulus by ~31%, a moderate, ~11% strength improvement and a 15% drop in energy to failure. The increase in elastic modulus is close to the rule of mixture predictions when considering the

CNF elastic modulus reported in figure 4. The loss in energy to failure merely indicates the loss in ductility by adding CNFs.

Replacing pristine CNFs with functionalized CNF as filler for the epoxy matrix does not change the elastic modulus, as evident figure 7(b), while it leads to enhancement in strength (21% improvement with respect to neat matrix), figure 7(c). Because the strengths in individual pristine and functionalized CNFs are nearly the same (figure 4), the higher strength and energy to failure found in nanocomposites with functionalized CNFs compared to pristine CNFs should be attributed to the enhanced interfacial load transfer facilitated by surface functional groups.

The nanocomposite's fracture surface provides more evidence to support the claim that there is weaker CNF-epoxy bonding in un-functionalized CNFs. Figures 7 (e) and (f) show the fracture surfaces for composite specimens containing functionalized and pristine CNFs in epoxy, respectively. A clear difference between the functionalized and pristine CNFs is that composite specimen containing pristine CNFs were more prone to form agglomerates compared to functionalized CNFs. The sites showing agglomerated CNFs are more numerous for the pristine CNFs/epoxy composite, an indication of weaker CNF-epoxy interaction that manifest itself in the lower tensile strength for nanocomposites with pristine CNFs.

4. Conclusion

Chemical functionalization, intended to enhance carbon nanomaterial interactions with a polymer matrix, may adversely affect the strength in individual nanomaterials by disrupting their graphitic structure. In this work, we evaluated the strength loss caused by functionalization in CNFs that are composed of a highly crosslinked network containing amorphous and graphitic carbon and compared that with the trend observed in nanomaterials with layered structures such as CNTs, as well as with carbon microfibers. Fracture strength estimations of the critical flaw size in CNFs, CNTs and graphene revealed that despite having a high surface area, carbon nanomaterials with crosslinked microstructure are resilient to flaws as big as 10–30 nm, while nanomaterials with layered structure (such as CNTs) experience a dramatic loss in strength with much lower flaw sizes (1–3 nm). Hence, it seems that the remarkably high-strength of graphitic nanomaterials such as graphene and CNT—with strengths that are higher than CNFs—come at a cost to flaw tolerance and structural robustness. In addition, comparing the strength of CNFs and carbon fibers with similar functionalization treatment revealed that the nanomaterials can be much more sensitive to acid treatment. This is attributed to the higher surface to volume ratio for nanomaterials that results in higher surface defects (oxidized sites) per unit volume.

In addition, a 1 wt% carbon nanofibers epoxy composite showed an improvement in the tensile strength when the CNFs are functionalized, compared to composites with pristine CNFs, because higher interfacial bonding between the CNFs and epoxy matrix is achieved by grafting functional

groups on the CNFs surfaces. Our current approach effectively enhanced the surface functional groups, without sacrificing mechanical properties in carbon nanofiber.

Acknowledgments

The authors acknowledge the support from Qatar National Science Funds, under the award number 8-2048-2-804. The use of the TAMU Materials Characterization Facility in TAMU is acknowledged. We also thank Dr. Svetlana Sukhishvili for using her lab facilities to perform the functionalization.

ORCID iDs

Jamshid Kavosi  <https://orcid.org/0000-0001-7303-0858>

Mohammad Naraghi  <https://orcid.org/0000-0002-1841-7598>

References

- [1] Peng B, Locascio M, Zapol P, Li S, Mielke S L, Schatz G C and Espinosa H D 2008 Measurements of near-ultimate strength for multiwalled carbon nanotubes and irradiation-induced crosslinking improvements *Nat. Nanotechnol.* **3** 626–31
- [2] Yu M F, Files B S, Arepalli S and Ruoff R S 2000 Tensile loading of ropes of single wall carbon nanotubes and their mechanical properties *Phys. Rev. Lett.* **84** 5552–5
- [3] Yu M F, Lourie O, Dyer M J, Moloni K, Kelly T F and Ruoff R S 2000 Strength and breaking mechanism of multiwalled carbon nanotubes under tensile load *Science* **287** 637–40
- [4] Lee C, Wei X D, Kysar J W and Hone J 2008 Measurement of the elastic properties and intrinsic strength of monolayer graphene *Science* **321** 385–8
- [5] Ramanathan T et al 2008 Functionalized graphene sheets for polymer nanocomposites *Nat. Nanotechnol.* **3** 327–31
- [6] Roy S, Petrova R S and Mitra S 2018 Effect of carbon nanotube (CNT) functionalization in Epoxy–CNT composites *Nanotechnol. Rev.* **7** 475–85
- [7] Young R J, Kinloch I A, Gong L and Novoselov K S 2012 The mechanics of graphene nanocomposites: a review *Compos. Sci. Technol.* **72** 1459–76
- [8] Ramanathan T, Stankovich S, Dikin D A, Liu H, Shen H, Nguyen S T and Brinson L C 2007 Graphitic nanofillers in PMMA nanocomposites—an investigation of particle size influence on nanocomposite and dispersion and their properties *J. Polym. Sci.* **45** 2097–112
- [9] Mikhalech A, Gspann T and Windle A 2016 Aligned carbon nanotube–epoxy composites: the effect of nanotube organization on strength, stiffness, and toughness *J. Mater. Sci.* **51** 10005–25
- [10] Cheng Q F, Wang J P, Wen J J, Liu C H, Jiang K L, Li Q Q and Fan S S 2010 Carbon nanotube/epoxy composites fabricated by resin transfer molding *Carbon* **48** 260–6
- [11] Tasis D, Tagmatarchis N, Bianco A and Prato M 2006 Chemistry of carbon nanotubes *Chem. Rev.* **106** 1105–36
- [12] Liao Y H, Marietta-Tondin O, Liang Z Y, Zhang C and Wang B 2004 Investigation of the dispersion process of SWNTs/SC-15 epoxy resin nanocomposites *Mater. Sci. Eng. A* **385** 175–81
- [13] Xiao T, Liu J and Xiong H 2015 Effects of different functionalization schemes on the interfacial strength of carbon nanotube polyethylene composite *Acta Mech. Solida Sin.* **28** 277–84

- [14] Zhang Z Q, Liu B, Chen Y L, Jiang H, Hwang K C and Huang Y 2008 Mechanical properties of functionalized carbon nanotubes *Nanotechnology* **19** 395705
- [15] Mielke S L, Troya D, Zhang S, Li J L, Xiao S P, Car R, Ruoff R S, Schatz G C and Belytschko T 2004 The role of vacancy defects and holes in the fracture of carbon nanotubes *Chem. Phys. Lett.* **390** 413–20
- [16] Zandiatahbar A, Lee G H, An S J, Lee S, Mathew N, Terrones M, Hayashi T, Picu C R, Hone J and Koratkar N 2014 Effect of defects on the intrinsic strength and stiffness of graphene *Nat. Commun.* **5**
- [17] Khoei A R and Khorrami M S 2016 Mechanical properties of graphene oxide: a molecular dynamics study *Fuller Nanotubes Carbon Nanostruct.* **24** 594–603
- [18] Drzal L T, Sugiura N and Hook D 1996 The role of chemical bonding and surface topography in adhesion between carbon fibers and epoxy matrices *Compos. Interfaces* **4** 337–54
- [19] Bahl O P, Mathur R B and Dhami T L 1984 Effects of surface-treatment on the mechanical-properties of carbon-fibers *Polym. Eng. Sci.* **24** 455–9
- [20] Beese A M, Papkov D, Li S Y, Dzenis Y and Espinosa H D 2013 In situ transmission electron microscope tensile testing reveals structure-property relationships in carbon nanofibers *Carbon* **60** 246–53
- [21] Papkov D et al 2013 Extraordinary improvement of the graphitic structure of continuous carbon nanofibers templated with double wall carbon nanotubes *ACS Nano* **7** 126–42
- [22] Chawla S, Cai J Z and Naraghi M 2017 Mechanical tests on individual carbon nanofibers reveals the strong effect of graphitic alignment achieved via precursor hot-drawing *Carbon* **117** 208–19
- [23] Chen Y, Amiri A, Boyd J G and Naraghi M 2019 Promising trade-offs between energy storage and load bearing in carbon nanofibers as structural energy storage devices **29** 1901425
- [24] Zussman E, Chen X, Ding W, Calabri L, Dikin D A, Quintana J P and Ruoff R S 2005 Mechanical and structural characterization of electrospun PAN-derived carbon nanofibers *Carbon* **43** 2175–85
- [25] Arshad S N, Naraghi M and Chasiotis I 2011 Strong carbon nanofibers from electrospun polyacrylonitrile *Carbon* **49** 1710–19
- [26] Gardea F and Lagoudas D C 2014 Characterization of electrical and thermal properties of carbon nanotube/epoxy composites *Composites B* **56** 611–20
- [27] Naraghi M and Chawla S 2014 Carbonized micro- and nanostructures: can downsizing really help? *Materials* **7** 3820–33
- [28] Krekel G, Hüttinger K J, Hoffman W P and Silver D S 1994 The relevance of the surface structure and surface chemistry of carbon fibres in their adhesion to high-temperature thermoplastics **29** 2968–80
- [29] Rana S, Alagirusamy R, Figueiro R and Joshi M 2012 Effect of carbon nanofiber functionalization on the in-plane mechanical properties of carbon/epoxy multiscale composites *J. Appl. Polym. Sci.* **125** 1951–8
- [30] Klein K L, Melechko A V, McKnight T E, Retterer S T, Rack P D, Fowlkes J D, Joy D C and Simpson M L 2008 Surface characterization and functionalization of carbon nanofibers *J. Phys. D: Appl. Phys.* **103** 061301
- [31] Gardner S D, Singamsetty C S K, Booth G L, He G R and Pittman C U 1995 Surface characterization of carbon-fibers using angle-resolved XPS and ISS *Carbon* **33** 587–95
- [32] Cai J and Naraghi M 2018 Non-intertwined graphitic domains leads to super strong and tough continuous 1D nanostructures *Carbon* **137** 242–51
- [33] Chen Y, Cai J, Boyd J G, Kennedy W J and Naraghi M 2018 Mechanics of emulsion electrospun porous carbon fibers as building blocks of multifunctional materials *ACS Appl. Mater. Interfaces* **10** 38310–18
- [34] Cai J Z, Chawla S and Naraghi M 2016 Microstructural evolution and mechanics of hot-drawn CNT-reinforced polymeric nanofibers *Carbon* **109** 813–22
- [35] Wu Z H, Pittman C U and Gardner S D 1995 Nitric-acid oxidation of carbon-fibers and the effects of subsequent treatment in refluxing aqueous NaOH *Carbon* **33** 597–605
- [36] Gao H, Ji B, Jäger I L, Arzt E and Fratzl P 2003 Materials become insensitive to flaws at nanoscale: lessons from nature *Proc. Natl. Acad. Sci.* **100** 5597–600
- [37] Ajori S, Ansari R and Haghghi S 2018 A molecular dynamics study on the buckling behavior of cross-linked functionalized carbon nanotubes under physical adsorption of polymer chains *Appl. Surf. Sci.* **427** 704–14
- [38] Erickson M and Kirk M 2017 Direct use of fracture toughness for flaw evaluations of pressure boundary materials in section XI, division 1, class 1 ferritic steel components *Proc. ASME Pressure Vessels and Piping Conf. 2017* vol 1a
- [39] Cao C H, Mukherjee S, Howe J Y, Perovic D D, Sun Y, Singh C V and Filleter T 2018 Nonlinear fracture toughness measurement and crack propagation resistance of functionalized graphene multilayers *Sci. Adv.* **4** eaao7202
- [40] Yang L, Greenfeld I and Wagner H D 2016 Toughness of carbon nanotubes conforms to classic fracture mechanics *Sci. Adv.* **2** e1500969
- [41] Ansari R, Ajori S and Rouhi S 2015 Structural and elastic properties and stability characteristics of oxygenated carbon nanotubes under physical adsorption of polymers *Appl. Surf. Sci.* **332** 640–7
- [42] Haghghi S, Ansari R and Ajori S 2019 Interfacial properties of 3D metallic carbon nanostructures (T6 and T14)-reinforced polymer nanocomposites: a molecular dynamics study *J. Mol. Graph. Model.* **92** 341–56